Supplementary Material for:

On-the-fly precision spectroscopy with a dual-modulated tunable diode laser and Hz-level referencing to a cavity

Shuangyou Zhang[a], Toby Bi[a,b], Pascal Del'Haye[a,b]*

[a]*Max Planck Institute for the Science of Light, Erlangen, 91058 Germany*

[b]*Department of Physics, Friedrich-Alexander-Universität Erlangen-Nürnberg, Erlangen, 91058, Germany*

Email: pascal.delhaye@mpl.mpg.de

Supplementary Note 1: FSR calibration based on dual RF modulation

When employing a single RF frequency at around half of the FSR, as depicted in Fig. S1(a), the laser scan speed (v_{scan}) is measured over the time interval (t_1 or t_2), resulting in a relatively large uncertainty on v_{scan}. On the other hand, when utilizing dual RF frequencies that are close to half the FSR, as shown in Fig. S1(b), the laser scan speed is computed nearly instantaneously over a much shorter time duration between the two sideband resonances (T_1 or T_2), which is approximately ten times smaller than the total FSR interval. This results in a more precise calculation of v_{scan}.

Furthermore, when using RF frequencies around multiples of FSR, ~(n+1/2)FSR, as illustrated in Fig. S1(c), the laser scan speed is calculated similarly to the dual RF case in Fig. S1(b) with same amount of uncertainty. However, the uncertainty of the calculated FSR is reduced by a factor of 1/(2n+1). Considering the availability in our lab, ~20 GHz is used for the modulation frequencies. This gives us a 1000 times improvement in determining the FSR of the reference cavity.

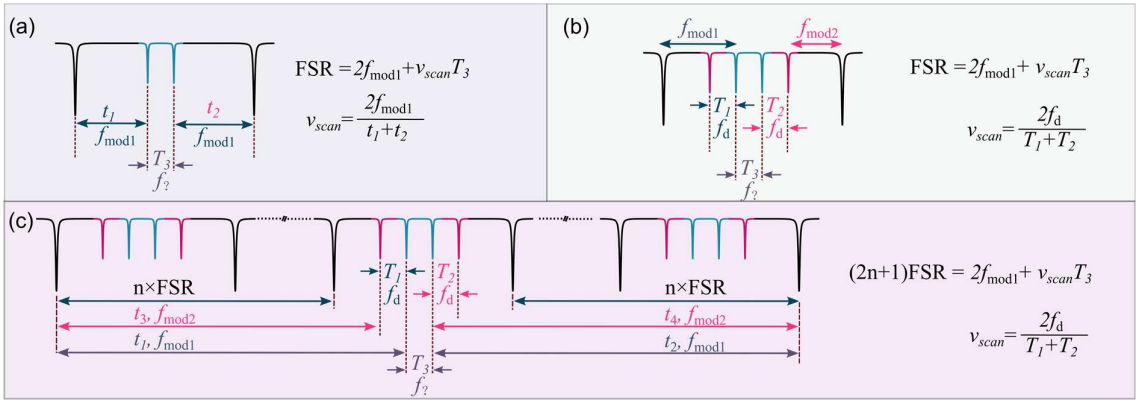

Fig. S1 Calculation of the FSR at different modulation frequencies. (a) Single modulation at approximately half the FSR. (b) Dual modulation at approximately half the FSR. (c) Modulation at larger frequencies corresponding to ~(n+1/2)×FSR.

Supplementary Note 2: Validation experiments using two 5-m fiber loop cavities

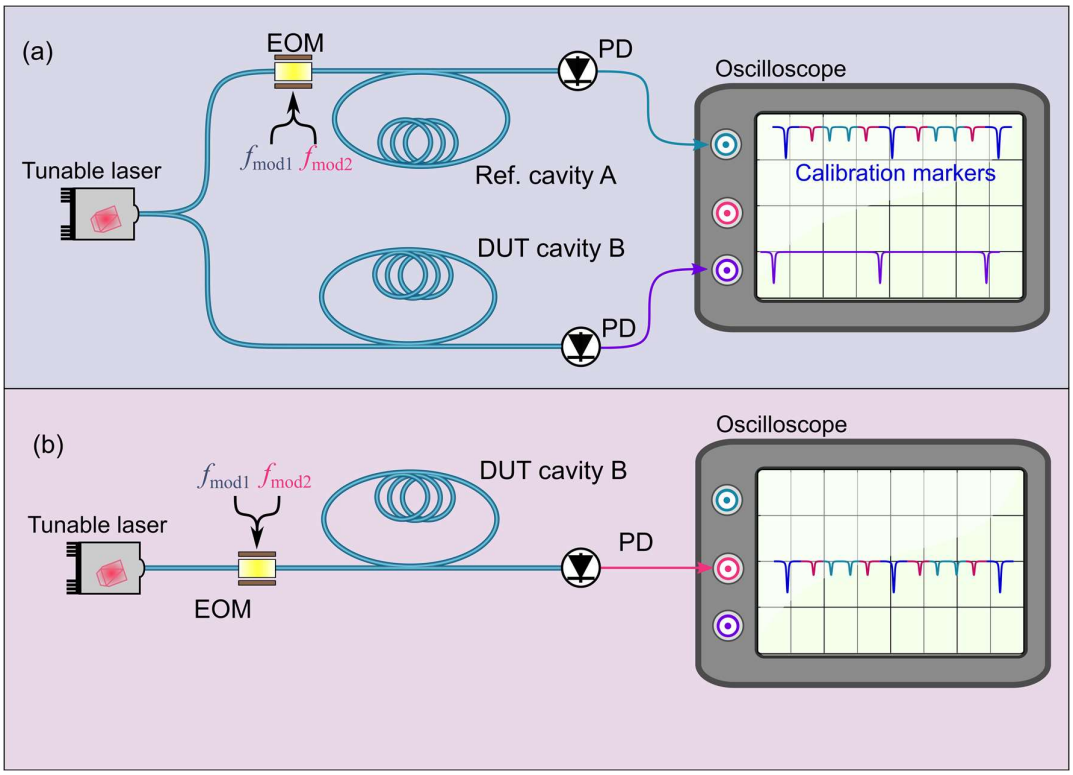

Fig. S2 Validation experiments using two independent 5-m fiber loop cavities. (a) the FSR of the cavity A is calibrated by the dual RF modulation scheme and used as the frequency reference to measure the FSR variation of cavity B across the O-band wavelength range. (b) the FSR of cavity B is measured independently by dual RF modulation to verify the measurement using reference cavity A in (a). Note that, due to the FSR frequency difference between the two fiber cavities, the modulation frequencies used in these two measurements are slightly different.

Figure S2 shows the experimental setup to verify our results using two 5-m fiber loop cavities (A and B) in two independent measurements. As shown in Fig. S2(a), for one measurement, we first use the dual RF modulation scheme to calibrate the FSR of fiber cavity A (FSR_A), while at the same time, the transmission of the under-test cavity B is recorded. The calibrated cavity A based on dual RF modulation is then used as the frequency reference to calculate the FSR of the cavity B (FSR_B). The results are plotted in Fig. S3(a). The red curve (right Y axis) shows the spectral variation of FSR_A with an value of ~38.941 MHz calibrated by dual RF modulation, while curve 1 (C1, blue, left Y axis) shows the variation of FSR_B using the polynomial fitted FSR_A as the frequency reference. Figure S3(b) shows the histogram of the frequency difference of the measured FSR_B (curve 1) in Fig S3(a), with respect to its second-order polynomial fitted values, showing a root-mean-square (rms) deviation of 9.0 Hz. This result independently verifies the precision of our spectroscopy method.

To verify the calculation of the FSR of cavity B in the first measurement, we directly measure it using dual RF modulation, as shown in Fig. S2(b). Note that, due to the FSR difference (40 kHz) between the two cavities, the modulation frequencies are different for these two experiments. The black curve (C2,

left axis) in Fig. S3(a) shows the evolution of the FSR of cavity B measured with dual RF modulation and is in excellent agreement with curve C1 that has been calibrated by the reference cavity A. By fitting both curves using second-order polynomial fits, Figure S3(c) shows the frequency difference between the two fitted curves. The frequency difference across the whole scan range is on the order of 10 Hz, which we speculate is due to temperature drifts of the fiber cavity between the two measurements. The thermal expansion coefficient of a single mode fiber is around 8 ppm/K[31], which corresponds to 15 Hz variation on the 39-MHz FSR for a 0.05-K temperature drift. This temperature variation is reasonable, considering our laboratory conditions.

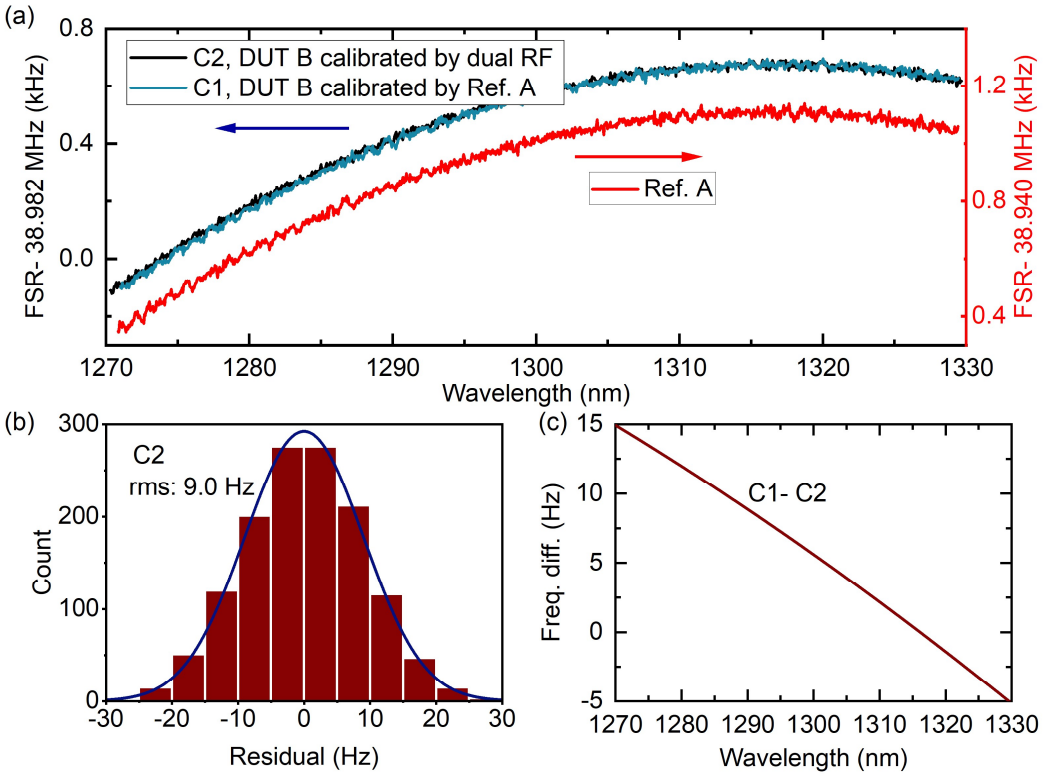

Fig. S3 FSR measurement of the fiber loop cavity B calibrated by two independent experiments. (a) FSR evolutions of cavity B measured using cavity A as reference (C1, blue, left axis), and calibrated using the dual RF modulation scheme (C2, black, left axis). The red curve (right axis) shows the FSR variation of the reference cavity A. Its second-order polynomial fitted values are used as the reference frequency. (b) Histogram of the frequency difference of the measured FSRs of cavity B (C1) in (a), with respect to its second-order polynomial fitted values, and a fitted Gaussian curve with a rms deviation of 9.0 Hz. (c) Frequency difference between the two fitted results of C1 and C2 using second-order polynomial function.

Table I compares the frequency calibration performance of fiber resonators or Mach-Zehnder interferometers (MZIs) used as frequency calibrators for tunable diode laser spectroscopy with the method proposed in this work. Compared to these methods, our work shows an improvement by one order of magnitude in terms of relative frequency precision. Additionally, our method stands out as being capable of on-the-fly calibration of the reference cavities, whereas other schemes measure the

reference at discrete wavelengths. Thus, our method offers higher robustness against environmental noise.

Table I Comparison of the frequency calibration performance of fiber resonators or Mach-Zehnder interferometers (MZIs) as frequency calibrators for tunable diode laser spectroscopy with the method proposed in this work.

	Bandwidth (THz)	Speed (THz/s)	Relative Precision (Precision/FSR)
Single sideband +MZI[19]	4	Discrete.	5.5×10^{-6}
Single sideband +MZI[44]	12	Discrete	2.4×10^{-3}
Precalibrated fiber cavity[15]	55	Discrete	2.0×10^{-6}
Single sideband + fiber cavity[45]	0.2	Discrete	1.8×10^{-3}
This work	11	1	2.1×10^{-7}

When we apply our method to HF gas spectroscopy or microresonator measurements with 100 GHz mode spacing, a scan across multiple FSRs of the reference cavity is used to determine the frequency distance between features under test. A simple and conservative estimate is that the error of the FSR of the reference cavity accumulates with increasing frequency distance. This would give us a relative precision of $2.1\text{x}10^{-7}$, corresponding to a 2.3 MHz uncertainty for an 11 THz frequency measurement. However, in our measurement, the FSR of the reference cavity vs. wavelength is fitted by a polynomial, and the fitted FSR values are used to determine the frequency distance between features under test. Since the FSR of the reference cavity evolves smoothly, we find that the error does not accumulate. To experimentally validate this claim, we employ two independent 5-m fiber cavities to calibrate the frequency scan of the tunable laser. As shown in Fig. S2(a), the dual-RF modulated tunable laser probes two 5-m fiber cavities (Cav. A and Cav. B) simultaneously while being tuned from 1270 nm to 1330 nm. The transmission of the two fiber cavities is recorded and used to convert the laser sweep time to frequency based on the FSR of each cavity, independently. The converted laser frequencies (FreqCavA and FreqCavB) are compared against each other, and the result is plotted in Fig. S4(a), showing an excellent agreement between two independently calibrated frequencies from 1270 nm to 1330 nm. The frequency difference scatters around zero, with an rms value of 220 kHz. The frequency difference does not increase with increasing frequency range. We achieve a precision of 220 kHz and a relative precision of 2.0×10^{-8} for a frequency range of 11 THz, which is limited by the tunable range of the laser used in the experiments. Please note that there are some relatively larger peaks in Fig. S4(a) due to the nonlinear frequency sweeping at the corresponding time. For example, Figure S4(b) shows the transmission traces

of two fiber cavities, corresponding to the spectral region marked in the dashed box in Fig. S4(a). It is evident that the laser is sweeping nonlinear, experiencing four different states: uniform scan rate, deceleration, then acceleration, deceleration, and finally back to uniform scan rate. Furthermore, we have performed additional experiments to study the reproducibility of these peaks. Our results show that these peaks are indeed rare and random, and their occurrence does not significantly affect the overall precision of the measurements. Thus these nonlinear scan ranges can be overcome by repeated measurements, ensuring the reliability and accuracy of the spectroscopy method.

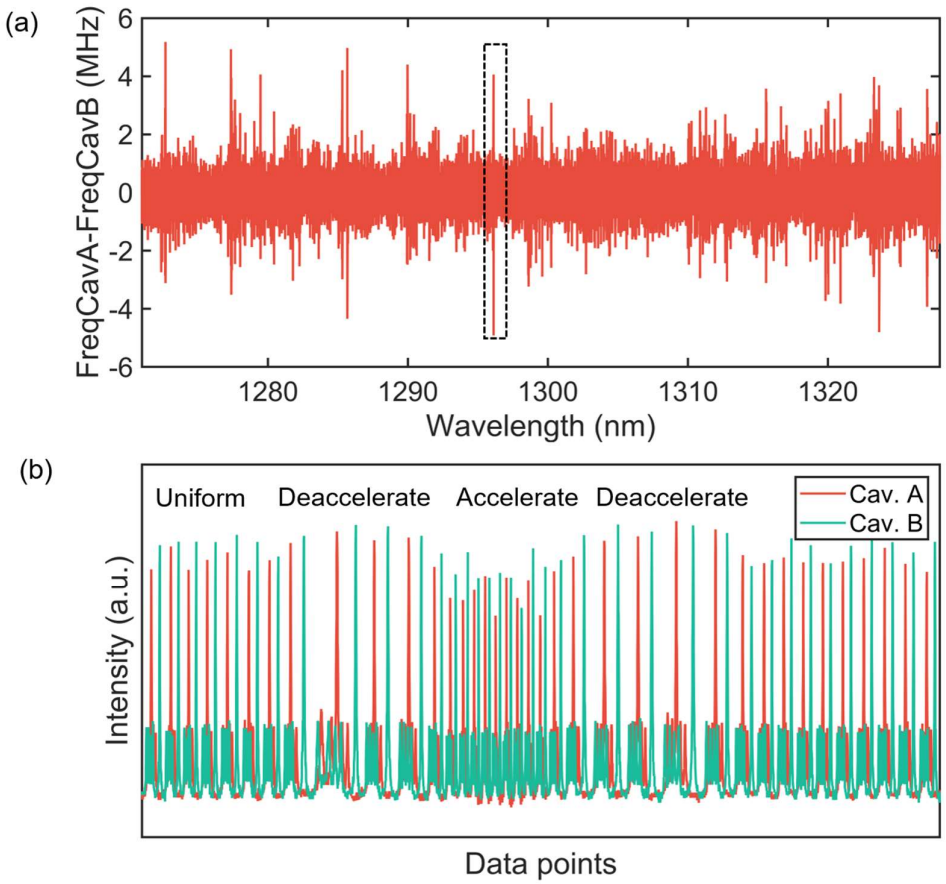

Fig. S4 Frequency comparison when the laser frequency is independently and simultaneously calibrated by two fiber cavities. (a) frequency difference between the calibrated laser frequencies by the two cavities. (b), transmission traces of two fiber cavities, corresponding to the spectral region marked by the dashed box in (a), showing a nonlinear laser sweeping.

Table II compares the performance of different tunable diode laser spectroscopy methods with our work in terms of bandwidth, precision, and measurement speed. Our method outperforms existing methods by two orders of magnitude in frequency precision while maintaining similar tuning speed and range.

Table II Comparison of typical tunable diode laser spectroscopy

	Resolution (MHz)	Bandwidth (THz)	Speed (THz/s)	Relative precision (Over entire reported tuning range)
Single sideband +MZI[19]	-	4	-	5.5×10^{-6}
Wavemeter[17]	2	8	0.5	4.6×10^{-4}
Precalibrated fiber cavity[15,a]	0.47	18.7	6.25	-
Optical channelestimation[18]	10	0.25	-	-
Interferometry[16]	200	13	8.3	2.5×10^{-2}
Single sideband modulation[36]	0.08	0.04	-	-
Comb assisted[20]	1	4	1	4.5×10^{-6}
This work	0.2	11	1	2.0×10^{-8}

[a,] we used the bandwidth (18.7 THz) for which the tuning speed (6.25 THz/s) is reported.

Supplementary Note 3: Measured absorption line positions and Lorentzian linewidths of HF gas

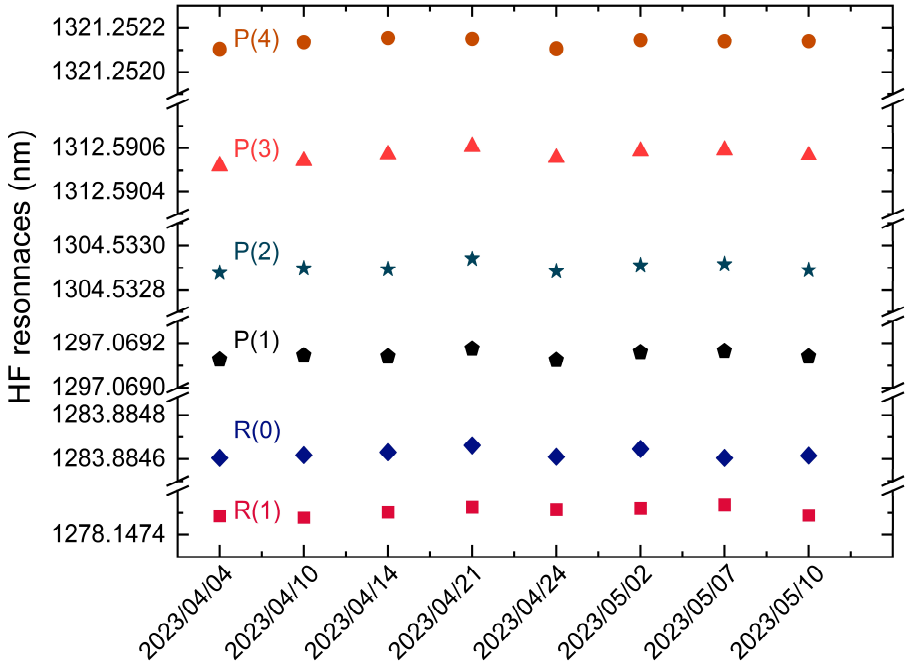

Fig. S5 Measured positions of HF absorption lines using the proposed dual-modulated tunable diode laser spectroscopy. These measurements were taken on different dates over the course of a month.

Figure S5 displays the measured positions of the HF molecular absorption lines (P and R branches) in the O-band range, obtained on various dates from April to May 2023. As stated in the main text, we utilize the R(2) absorption line as the absolute frequency reference, setting it equal to the calculated value (1272.97025 nm) from the HITRAN database. The statistical analysis shows our measurement with an uncertainty of ~ 0.02 pm. Taking P(4) as an example, the Voigt fit uncertainties for both R(2) and P(4) lines are 2.1 MHz and 2.4 MHz, respectively. The frequency distance between the R(2) and P(4) lines is 8.6 THz. As discussed above, for the measurement of the relative frequency position, the FSR error of the reference cavity does not accumulate with the increase of the measurement frequency range. The uncertainty of the 8.6 THz frequency distance is around 220 kHz, which is way smaller than that caused by the Voigt fit. Thus, considering the uncertainty from both Voigt fits, the uncertainty of the spacing between HF absorption lines can be evaluated to be around 4 MHz. This agrees well with the experimental measurement, where P(4) is determined with an uncertainty of 3.3 MHz (0.02 pm). Other factors on the frequency uncertainty of the P(4) line are also evaluated and summarized in the table below. Considering a temperature drift of 0.01 K in 10 s measurement time, this induces around 688 kHz uncertainty for an 8.6 THz frequency distance, using the thermal expansion coefficient of a single mode fiber, which is around 8 ppm/K[31]. The RF signal used for the dual modulation is referenced to a Rubidium clock with an accuracy of 5×10^{-11}, resulting in an uncertainty of 430 Hz. Figure S6 shows the wavelength difference ($\Delta\lambda$) between the measured line positions and the calculated values based on HITRAN database. The measured line positions are at slightly shorter wavelengths than the calculated

values, which may be attributed to the pressure of the gas cell being higher than the specified value of 50 Torr (see discussion below).

Table III Uncertainty analysis of HF P(4) line

Effects	Uncertainty (MHz)
Fit uncertainty	2.4
Temperature	~0.7
RF modulation signal	0.0004
Laser linewidth	0.01
Reference cavity	0.2

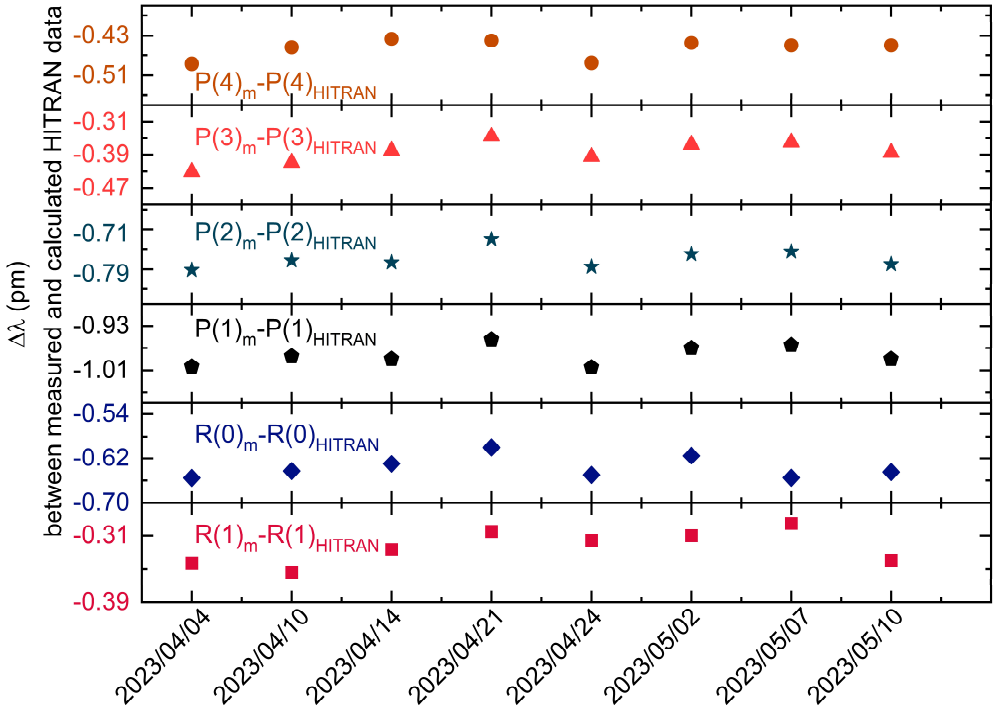

Fig. S6 Wavelength difference between the experimentally measured positions of HF absorption lines (shown in Fig. S5) and the calculated wavelengths based on HITRAN. The suffix 'm' in the figure means measured.

Figure S7 shows the measured Lorentzian linewidths of HF gas line, obtained on the same dates as in Fig. S5. The Lorentzian linewidths are calculated by using a Vogit fit function and calucaled Gaussian linewidth in Table 1 in the main text. The uncertainty of the linewidth measurement is on the order of ten MHz.

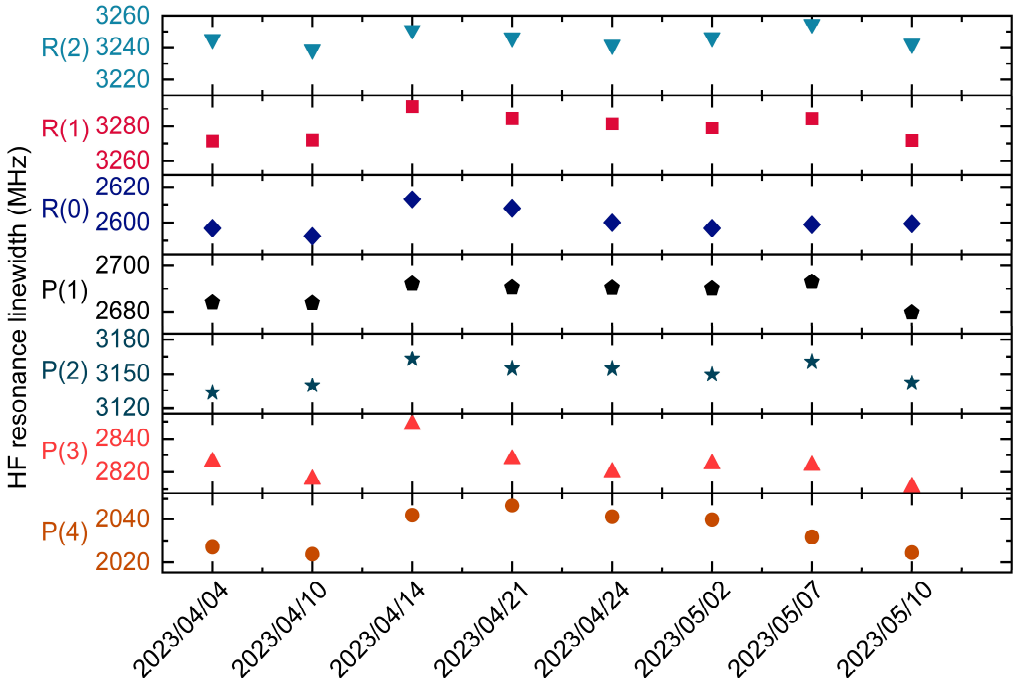

Fig. S7 Experimentally measured Lorentzian linewidths of HF absorption lines. These results are obtained from same set of measurements used in Fig. S5 and S6.

Supplementary Note 4: HF linewidth measurement validated by the sideband spectroscopy

Figure S8(a) shows the experimental setup used to measure the linewidth of HF absorption lines in the O-band wavelength range. Rather than using the motor for wide laser frequency scanning (11 THz) as in the main text, in the sideband spectroscopy, the laser frequency is first tuned close to each absorption resonance of the HF gas and then the laser frequency is swept via the piezo in a small frequency range (~ 40 GHz) to observe the HF absorption lines at different wavelengths. The laser frequency scanning is calibrated by modulating the optical frequency using an EOM driven by a 10-GHz RF signal, resulting in two additional absorption lines from the generated optical sidebands in the time domain with a known frequency separation equal to the 10-GHz modulation. For instance, Figure S8(b) shows the P(4) absorption line with two additional absorption lines from the modulated optical sidebands. Based on this time-to-frequency calibration, the Lorentzian FWHM linewidth of each absorption line is calculated using the Vogit function and the calculated Gaussian linewidth in Table 1 in the main text.

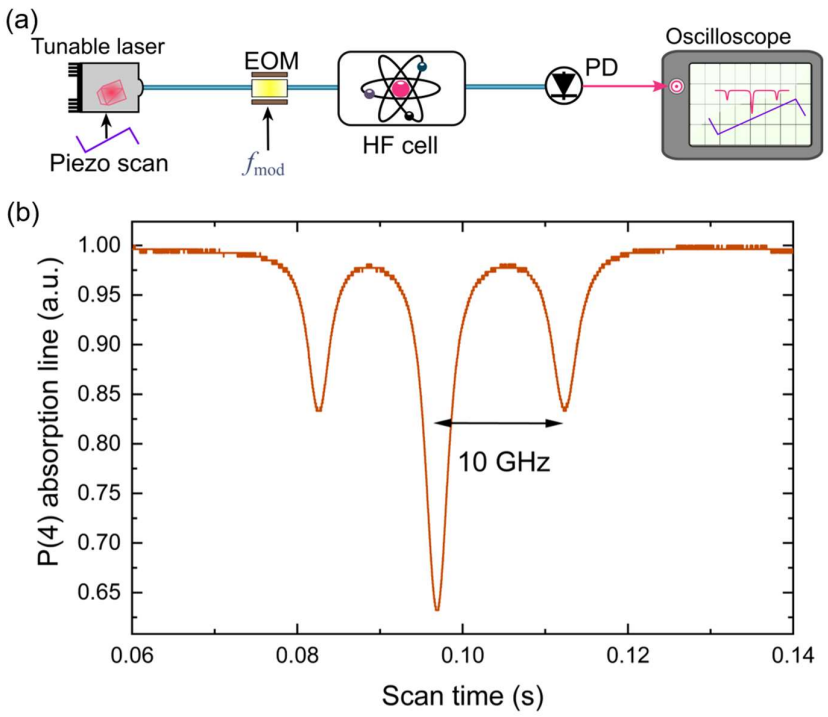

Fig. S8 HF linewidth measurement validated by the sideband spectroscopy. (a) Experimental setup for measuring the linewidth of the HF absorption lines. (b) P(4) absorption line with two additional absorption lines from the modulated optical sidebands spaced by 10 GHz.

By using this method, the linewidth of the HF absorption line can be independently measured to verify the results obtained by the dual-modulated tunable diode laser spectroscopy presented in the main text. Figure S9 shows a comparison of the Lorentzian linewidth measurement using these two methods, along with the calculated Lorentzian linewidth from the HITRAN database. It can be observed that the two methods are in a good agreement with each other. Thus, the measured Lorentzian linewidth from both methods is consistently larger than the calculated value, providing additional evidence that the pressure in the HF gas cell is slightly higher than the 50 Torr specified by the manufacturer.

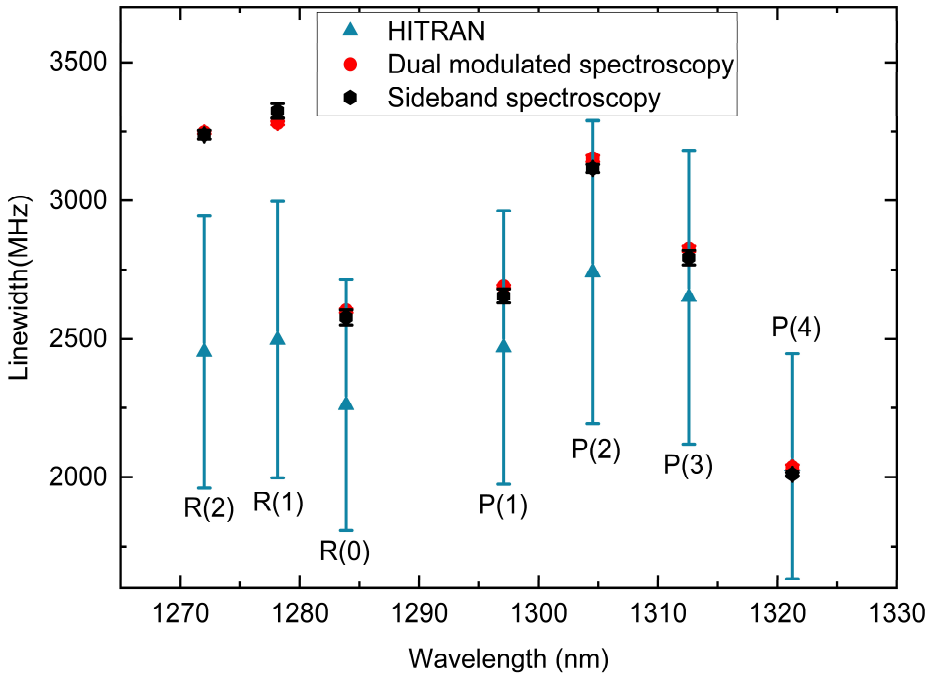

Fig. S9 Comparison of the Lorentzian linewidth measurement using sideband spectroscopy (black hexagon) via pizeo scanning of laser frequency and dual-modulated tuanble diode laser spectroscopy (red circle) via motor scanning over 11 THz range, along with the calculated Lorentzian linewidth (blue triangle) from the HITRAN database. The uncertainty of the Lorentzian linewidth is calculated based on 20% uncertainty of the gas pressure, specified by the gas cell manufacturer.